



ACADÉMIE  
DES SCIENCES  
INSTITUT DE FRANCE

# *Comptes Rendus*

---

## *Physique*

Stavros Koulouridis


**Implantable  $T_x$ - $R_x$  wireless systems. An overview of their efficiency analysis through scattering matrix formalism**

Published online: 7 November 2024

**Part of Special Issue:** Energy in the heart of EM waves: modelling, measurements and management

**Guest editors:** Emmanuelle Conil (ANFR, France), François Costa (ENS Paris-Saclay, Université Paris-Saclay, Université Paris-Est Créteil, France) and Lionel Pichon (CNRS, CentraleSupélec, Université Paris-Saclay, Sorbonne Université, France)

<https://doi.org/10.5802/crphys.208>

 This article is licensed under the  
CREATIVE COMMONS ATTRIBUTION 4.0 INTERNATIONAL LICENSE.  
<http://creativecommons.org/licenses/by/4.0/>



*The Comptes Rendus. Physique are a member of the  
Mersenne Center for open scientific publishing*  
[www.centre-mersenne.org](http://www.centre-mersenne.org) — e-ISSN : 1878-1535



Review article / *Article de synthèse*

Energy in the heart of EM waves: modelling, measurements and management / *L'énergie au cœur des ondes électromagnétiques : modélisation, mesures et gestion*

## Implantable $T_x$ – $R_x$ wireless systems. An overview of their efficiency analysis through scattering matrix formalism

*Systèmes implantables sans contact. Analyse de l'efficacité du transfert par le formalisme de la matrice de diffusion*

Stavros Koulouridis<sup>®,<sup>a</sup></sup>

<sup>a</sup> University of Patras, 26504, Rio-Patra, Greece

E-mail: stavros.koulouridis@upatras.gr

**Abstract.** Looking at wireless implantable systems as a pair of or more  $T_x$ – $R_x$  components, we discuss how their efficiency can be calculated in order to achieve an optimum result that can be evaluated over measurements and literature. To that end, scattering parameters' notation is introduced instead of considerations of the gain, the propagation losses and the radiation patterns. Looking at the system as a black box, remarks on optimum link calculation in relation to frequency, antenna size, phantom use, matching circuit integration and efficiency intensifiers are being carried out. International standards for allowed power and safety levels are added to the discussion. Different scenarios including telemetry, wireless harvesting and sensor transmission information are included as examples.

**Résumé.** En considérant un système implantable sans contact comme une paire de composants  $T_x$ – $R_x$  (émetteur-récepteur), l'article montre que l'efficacité de transfert peut être calculée en vue d'obtenir un résultat optimal pouvant être évalué au moyen de mesures ou de résultats issus de la littérature. À cette fin, le formalisme des paramètres S (matrice de diffusion) est introduit à la place des quantités généralement utilisées (gain, pertes, diagramme de rayonnement). En considérant le système comme une boîte noire, des remarques sur le calcul de la liaison optimale sont formulées selon la fréquence, la taille de l'antenne, l'utilisation d'un fantôme, l'intégration de circuits d'adaptation et d'amplificateurs d'efficacité. Les normes internationales relatives à la puissance autorisée et aux niveaux de sécurité à respecter sont incluses dans la discussion. Différents scénarios incluant la télémétrie, la récupération d'énergie sans fil et la transmission d'informations par des capteurs sont présentés à titre d'exemples.

**Keywords.** Scattering parameters, Friis equation, Link budget, SAR, Wireless harvesting systems.

**Mots-clés.** Paramètres S, Equation de Friis, Bilan de liaison, DAS (débit d'absorption spécifique), Récupération d'énergie sans fil.

**Note.** This article follows the URSI-France workshop held on 21 and 22 March 2023 at Paris-Saclay.

*Manuscript received 22 May 2024, revised 12 August 2024, accepted 13 September 2024.*

## 1. Introduction

Significant research has been focused on studying, realizing, and implementing wireless body area networks. Applications include among others implantable devices for vital data recording, cameras that wirelessly transmit low-bit images, or wireless energy harvesting systems for unobtrusive and sustainable implantable sensors. For example, continuous non-invasive glucose measurements can help diabetes patients [1]. Under a usual scenario, an implantable device will obtain measurements, it will transmit them to an external relay through an antenna, and the relay will transmit the information to a party of “interest”, like a patient, hospital or a doctor.

Electromagnetic propagation inside the lossy inhomogeneous body which is composed of various organs of different electric properties causes increased absorption in the body. In addition, the complex environment introduces multiple reflections that can derange expected antenna performance. In addition, the inhomogeneous body structure has an effect on antenna behavior since it creates impedance mismatches. In effect the antenna radiation properties are affected by the body and the optimum performance of an implantable antenna design is not a straightforward process.

Research has considered several frequency bands for implantable sensors' design. Higher frequencies permit the use of larger electrical designs (while being physically small). However, when the depth increases, the higher frequencies lead to increased losses, even higher than the theoretically predicted ones [2]. In some cases, the large distances between an external relay and the implantable antenna makes obligatory the use of smaller frequencies. Of course, the frequency selection is also related to the specific scenario examined. Dual (or triple) frequency implantable systems can be also proposed, sending a wake signal at higher frequency and relaying medical information at lower frequency [3], or using a higher frequency where nominally higher power is permitted for wireless energy transfer [4, 5]. Interestingly, when ideal scenarios are considered, an optimum frequency for the implantable antenna can be determined [6]. However, when some of the parameters are altered, optimum design frequency can actually change.

Wireless Power Transfer systems introduce additional complexity in the implantable sensor design. First, their use can allow, in some cases, for battery-less designs or, in general, avoiding use of wires. Still, a rectenna is to be used, meaning that the receiving antenna needs to be connected to a rectifying circuit and sometimes voltage boosters or other electronic components [5]. In such cases, the antenna is coupled with the circuit and its design is seen as a single component, i.e., the “rectenna”, which introduces additional design parameters but also adds degrees of freedom in the final device.

In other cases, extra components are introduced in addition to the implantable antenna. For example, external “facilitators” that are applied to the body and can increase implantable antenna reception or the link with an external antenna are proposed. Or, more than one implantable antenna may be considered that needs to communicate or relay information to other components, etc.

Obtaining the optimum design is hence a complex process that can be affected by different factors. In order to simplify the study and also offer a measure of achievement, the use of scattering matrix can be introduced. In that case, we study a system that has two ports and includes the implanted and the external antenna, the multiple implanted antennas or all the components that constitute the design. In the end the system has two ports, one input and one output, that can be used to evaluate the system efficiency and determine its performance. The simulations can be directly compared with measurements and with several designs in the literature.

In this paper, after a short introduction into scattering parameters use for the system under consideration, we determine how the system efficiency can be calculated for two cases. When simply two antennas (Section 2.1) are used and when additional circuits connected to the antennas are considered in the case of harvesting systems for example (Section 2.1.1). Link budget considerations follow for telemetry systems. International restrictions for wireless systems used in implantable designs are then presented, accompanied by power limitations as reported in international standards. Some examples are discussed in Section 3. First, we briefly discuss about ideal frequency for optimum efficiency when two implantable antennas are communicating with each other. Then, we examine how antenna size and radiation pattern can affect efficiency by analyzing four implantable microstrip antennas operating at MedRadio Band (400 MHz region). This region is selected, since it seems to be ideal for deeply implantable systems. When maximum allowed power for antennas is also considered, discussion for optimum frequency is then carried out, in order to close a link between an external antenna and an implantable antenna as is required for telemetry systems. Next, a couple of rectennas is considered in order to present an example of the necessity to include circuits in the scattering matrix consideration. Section 3 ends with a short comment on how added surfaces, on the skin, can increase the system efficiency. Some very simple solutions are presented in comparison with much more sophisticated ones based on metasurfaces for example. Finally, some conclusions are drawn in Section 4.

## 2. System overview

While the implantable antenna design demands considerable efforts, in order to evaluate the proposed setup performance, the problem needs to be examined as a system composed of two, three or multiple components. In a system design point of view, the implantable and the external antennas or multiple implantable antennas will be part of a two-port system represented by the well-known scattering  $S$ -parameters [7] as shown in Figure 1. In that system, the communication between two antennas can be one scattering matrix with individual scattering parameters, and the intercommunication between antenna pairs can be represented by a total scattering matrix which has been produced by a chain of separate scattering matrices. Selection of the system under examination relates to the problem under investigation. In any case, we can choose port 1 to be  $T_x$  antenna's feeding point and port 2 to be  $R_x$  antenna's ( $R_x$ ) reception point. In a multi antenna system, one antenna would be the  $T_x$  antenna and one other would be the  $R_x$  antenna, while the others could be intermediate parts of the system. The scattering  $2 \times 2$   $S$ -matrix which is generated represents the path link between the two antennas independently of what lies between them. Their input impedance is also included as part of the scattering matrix. Notably, in such a setting the two antennas system is the same for examining the reception/transmission of data or a wireless harvesting setup. Furthermore, the in-between distance (near, intermediate or far-field conditions) does not affect the system overview. Hence, the coupling between the antennas is also included in the matrix. While the  $S$ -matrix should be symmetric for a passive and/or linear element system, let us assume that, in general, we can have an asymmetric system, where non-linear components can be integrated into the system, and therefore:

$$S = \begin{bmatrix} S_{11} & S_{12} \\ S_{21} & S_{22} \end{bmatrix} \quad (1)$$

where  $S_{12} \neq S_{21}$  and of course  $S_{11} \neq S_{22}$  since the two antennas can be different.  $S$ -parameter matrix can be obtained from an electromagnetic solver and/or measurements for the fabricated system. Notably, comparison between measurements and simulations can be straightforward, adding another advantage on using  $S$ -parameters. The final  $2 \times 2$  scattering matrix, representing either each itemized link or the total link, will be connected to a load (either the  $R_x$  antenna

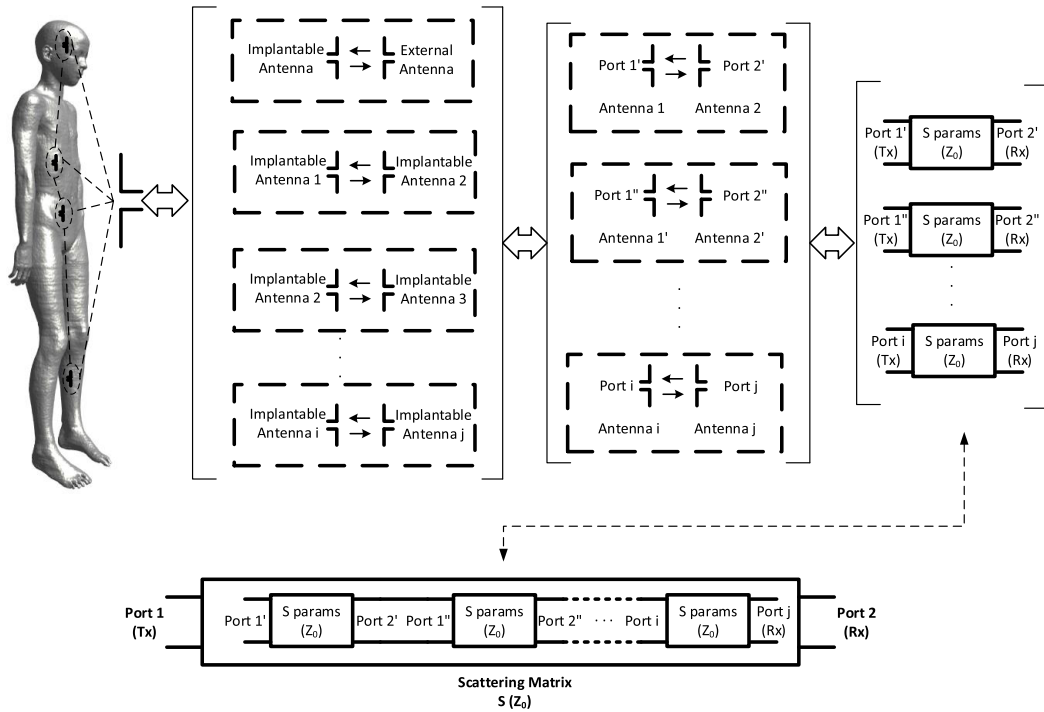


**Figure 1.** Communication link between implantable antennas or implantable antennas and external antenna replaced by one or more scattering matrices. Each scattering matrix can represent an antenna pair. The interconnection between the antenna pairs can be replaced by a chain of scattering matrices, or at the end by a total scattering matrix.

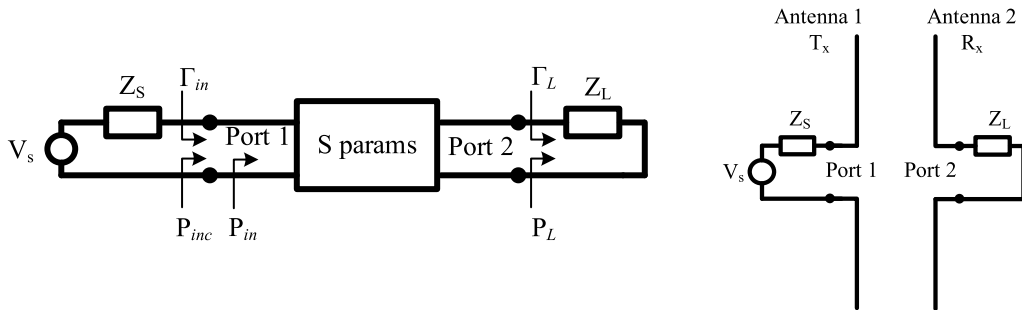


**Figure 2.** S-parameter circuit of an antenna pair with voltage source and termination load.

termination or another circuit) and will be fed by a voltage source with its internal impedance. This is shown in Figure 2.

### 2.1. Evaluation of system efficiency

In order to calculate the power received from the external or the implantable antenna, the well-known Friis formula can be utilized. This predicts the power received from an antenna in relation

to the power radiated from a transmitting antenna, their gain, path loss, antennae's matching and polarization. It is given by the following equation.

$$P_r = \frac{\lambda^2}{(4\pi r)^2} \cdot G_r \cdot G_t \cdot (1 - |S_{11}|^2) \cdot (1 - |S_{22}|^2) \cdot \text{PLF} \cdot P_t \quad (2)$$

where  $P_r$  and  $P_t$  are the power received and transmitted respectively,  $G_r$  and  $G_t$  are the antennas' received and transmitted realized gain respectively,  $\lambda$  is the wavelength of the intermediate medium,  $r$  is the in-between distance and PLF is the polarization factor (equal to 1 when the antennas are for example aligned and linearly polarized). It should be noted that the first product term and especially the wavelength/distance term (i.e.,  $\lambda^2/(4\pi r)^2$ ) expresses the free space (inside air or in a homogeneous infinite material) path loss, representing a spherical plane wave. Hence, far-field conditions and unobtrusive, free of hurdles, propagation should be observed. When an implantable antenna is for example receiving signal from an external transmitter the electromagnetic wave propagates into air and the body while multiple reflections are occurring as the signal passes through the complex body environment. To take into account non-ideal propagation (but without being able to avoid the far-field restriction) the above equation can be transformed into

$$P_r = \frac{\lambda^2}{(4\pi)^2} \left(\frac{1}{r}\right)^\gamma \cdot G_r \cdot G_t \cdot (1 - |S_{11}|^2) \cdot (1 - |S_{22}|^2) \cdot \text{PLF} \cdot P_t \quad (3)$$

Index  $\gamma$  can have theoretically any value from 1 to infinity. For implantable antenna systems values are definitely higher than 2. Index  $\gamma$ , in implantable antenna problems is obtained via simulation or measurements since no theoretical model exists. The process involves the curve fitting of measurements obtained at variable distances [8]. The outcome is unique to the system under investigation. Defining the path loss exponent can be of course useful but, in reality, it cannot offer a better overview of how well the pair implantable antenna/external antenna operates.

Equation (2) permits us to focus on the parameters that affect the reception of an antenna. These are the transmitting antenna gain, the receiving antenna gain, the matching of each antenna, the path losses that occur between the transmitting and receiving antenna and of course their polarization mismatch. While using Equation (2), would make the case ideal, in reality it is easily understood from the above discussion that in the case of implantable antenna and external transmitter, the predicted received power is simply the highest achievable [9], and there can be many factors that can affect this link. Since we are interested in estimating how well the system implantable antenna/external antenna behaves, we should actually use the scattering parameters of S-matrix. From the scattering parameter theory [7], it is very easily understood that:

$$|S_{21}|^2 = \frac{P_r}{P_t} \quad (4)$$

In that case from Equation (2)

$$|S_{21}|^2 = \frac{\lambda^2}{(4\pi r)^2} \cdot G_r \cdot G_t \cdot (1 - |S_{11}|^2) \cdot (1 - |S_{22}|^2) \cdot \text{PLF} \quad (5)$$

It is easily understood that efficiency  $n$  of the system is expressed by the ratio of received power  $P_r$  over the transmitted power  $P_t$ . Then:

$$n = |S_{21}|^2 \quad (6)$$

where  $|S_{21}|^2$  can be calculated by Equation (5). However, it might be more useful, sometimes, to calculate a slightly altered efficiency where the mismatch has been removed from the

calculations. This would be useful in the case we would like to study how the intermediate path can affect the system. Indeed, if we transform Equation (5) into:

$$\frac{|S_{21}|^2}{(1-|S_{11}|^2) \cdot (1-|S_{22}|^2)} = \frac{\lambda^2}{(4\pi r)^2} \cdot G_r \cdot G_t \cdot \text{PLF} \quad (7)$$

the right part refers to the system path loss, antenna gain and polarization factor and therefore it can actually reveal how the antenna gain (which can be affected by the surrounding complex environment) and the losses in between can affect the system “efficiency”  $n'$ . In that case we can write

$$n' = \frac{|S_{21}|^2}{(1-|S_{11}|^2) \cdot (1-|S_{22}|^2)}. \quad (8)$$

Notably, in order to have equivalency with the circuit of Figure 2 we should note that received power  $P_r = P_L$  when  $Z_L = Z_0$  while transmitted power  $P_t$  is equal to the power provided by a source at the  $T_x$  antenna input, that is  $P_t = P_{in}$ .

### 2.1.1. Evaluation of system efficiency at load. Use of matching circuits

The system efficiency calculations at the antenna point do not consider the power offered to the system, or the power that would be delivered to a load attached at the  $R_x$  system component. In addition, it does not take into account the use of antenna input impedance in order, for example, to match the antenna to a harvesting circuit or other kind of circuits implemented in the design. With reference to Figure 2, the efficiency can be calculated from [3, 10, 11]:

$$n = \frac{P_L}{P_{in}} = \frac{P_L}{(1-|\Gamma_{in}|^2)P_{inc}} = \frac{|S_{21}|^2(1-|\Gamma_L|^2)}{(1-|\Gamma_{in}|^2)(1-|S_{22}\Gamma_L|^2)} \quad (9)$$

where  $P_L$  is the power delivered to the load of the receiving antenna and  $P_{in}$  is the power offered to antenna.  $\Gamma_{in}$  is the reflection coefficient at port 1 and is equal [7] to

$$\Gamma_{in} = S_{11} + \frac{S_{12}S_{21}\Gamma_L}{1-S_{22}\Gamma_L} \quad (10)$$

and  $\Gamma_L$  is the reflection coefficient at the load calculated by

$$\Gamma_L = \frac{Z_L - Z_0}{Z_L + Z_0}. \quad (11)$$

The  $S$ -matrix can include, for example, the  $T_x$  antenna with a matching circuit and the  $R_x$  antenna which is connected to a harvesting circuit that will feed the load  $Z_L$ . It is noted that the  $S$ -matrix can be obtained for characteristic impedance  $Z_0 = 50 \Omega$ . Still, the antenna input impedance can differ from the ideal  $Z_0$ . The ultimate criterion for such a design is always the maximization of the system efficiency. In addition, by relaxing the antenna input impedance requirements, we can seek much more efficient harvesting circuits.

## 2.2. Link budget for wireless communications

For some scenarios that require telemetry or generally consider the transmission of information, the link budget needs to be considered. Link budget should consider the antenna losses, path losses, required bit rate, antenna gain, etc. Power input is controlled by electromagnetic compatibility safety standards for maximum power absorption from the tissues and electromagnetic interference avoidance and it varies with frequency and antenna size. In order to secure a communication link, one needs to achieve a positive carrier-to-noise density ratio  $C/N_0$  budget.  $C/N_0$  describes the strength of the power wave related to the noise. In Table 1, an example link budget is shown, including parameters to examine and indicative specifications of a satisfactory communication link [12, 13].

**Table 1.** Link budget parameters

Component	Description	Notation	Formula/data
Transmitter T <sub>x</sub>	T <sub>x</sub> Power (dBW)	$P_{Tx}$	
	Cable/feeding losses (dB)	$L_{Tx}$	
	T <sub>x</sub> Antenna gain (dBi)	$G_{Tx}$	
Propagation	Frequency	$f$	
	Space path loss (dB)	$P_{Loss}$	$10\log_{10}\left(\frac{(4\pi)^2}{\lambda^2} r^\gamma\right)$
Receiver R <sub>x</sub>	R <sub>x</sub> Power (dBW)	$P_{Rx}$	
	Cable/feeding losses (dB)	$L_{Rx}$	
	R <sub>x</sub> Antenna gain (dBi)	$G_{Rx}$	
	Ambient temperature (K)	$T_0$	293
	Boltzman constant	k	$1.38 \times 10^{-23}$
	Noise figure (dB)	NF	2.5
Signal quality	Noise power density (dB/Hz)	$N_0$	-201.7
	Bit Rate (b/s)	$B_r$	$10^6$
	Bit error rate	BER	$1 \times 10^{-5}$
	$E_b/N_0$ (ideal PSK) (dB)	$E_b/N_0$	9.6
	Coding gain (dB)	$G_c$	0
	Fixing deterioration (dB)	$G_d$	2.5

Cable/feeding losses in Table 1 include mismatch losses as a positive number. In the same manner, space path losses have been reversed since they should be retracted from final link budget. Equations to calculate the required link budget follow:

$$N_0 = 10\log_{10}(k) + \log_{10}(T_i) \text{ (dB/Hz)} \quad (12)$$

$$T_i = T_0(NF - 1) \text{ (K)} \quad (13)$$

$$\text{Achievable link } C/N_0 = P_{Tx} - L_{Tx} + G_{Tx} - P_{Loss} + P_{Rx} - L_{Rx} + G_{Rx} - N_0 \text{ (dB/Hz)} \quad (14)$$

$$\text{Required link } C/N_0 = \frac{E_b}{N_0} + 10\log_{10}(B_r) - G_c + G_d \text{ (dB/Hz)}. \quad (15)$$

For a successful link we should have a positive margin (dB) where this is given by Equation (16)

$$\text{Margin} = \text{Achievable link } C/N_0 - \text{Required link } C/N_0 \text{ (dB)}. \quad (16)$$

When the  $S$  scattering matrix is used, the link budget can be also calculated. In that case,  $S_{21}$  parameter will include all losses and gain occurred as can be easily seen by Equations (2)–(4). In that case,  $S_{21}$  in dB will be given by

$$S_{21} = G_{Tx} - L_{Tx} - P_{Loss} - L_{Rx} + G_{Rx} \text{ (dB)}. \quad (17)$$

And the Achievable and Required Link Budgets, considering Equation (4), will be finally:

$$\text{Achievable link } C/N_0 = P_{Tx} + S_{21} + 201.7 \text{ (dB/Hz)} \quad (18)$$

$$\text{Required link } C/N_0 = 72.1 \text{ (dB/Hz)}. \quad (19)$$

### 2.3. Frequency, safety and radiated power

Implantable devices and systems are mainly developed in sub-GHz or a few GHz region. While mm waves have been employed for wearable devices, this is not preferred for the embedded



**Table 2.** Typical medical frequencies for implantable devices

NameTag	Frequency (MHz)	ERP (dBm)	Reference
MedRadio	401–406	–16	[14–16]
	413–419	–16 <sup>a</sup>	[14]
	426–432	–16 <sup>a</sup>	[14]
	438–444	–16 <sup>a</sup>	[14]
	451–457	–16 <sup>a</sup>	[14]
	2360–2400	–16 <sup>a</sup>	[14]
Wireless medical telemetry service (WMTS)	608–614	31.8	[17]
	1395–1400	31.8	[17]
	1427–1432	31.8	[17]
Industrial, scientific and medical services band/ISM	433.05–434.79	10	[18]
	863–870	14	[18]
	902–928	30 (36 EIRP)	[19]
	2400–2484	30 (36 EIRP) <sup>b</sup>	[19]
	5725–5875	30 (36 EIRP) <sup>b</sup>	[19]

<sup>a</sup> It is assumed that it is incorporated from the main restriction for 401–406 MHz region.

<sup>b</sup> In general, EIRP can be larger for specific cases [19].

into tissue systems because of high absorption losses. The device development is regulated by several organizations around the world. Low MHz and kHz region has been used for inductive wireless charging and animal tags. However, wireless device development for communication is not practical and it is not considered in such low frequencies.

The main restriction for wireless implantable communication systems, apart from the operating frequency, is the maximum emitted power. It should be noted that this restriction is not necessarily related to the safety of the user but mostly to avoiding electromagnetic interference issues. Two quantities are usually used. ERP or Effective Radiated Power which represents the power fed to a matched antenna, and Equivalent Isotropically Radiated Power or EIRP which represents the maximum power radiated from an antenna, that is the power fed to matched antenna (in Watts) times the antenna gain over isotropic radiator. In an overview of the frequencies (Table 2), it is seen that specific frequencies have very low power limit. In that case the main goal is to perform close distance communication. In other cases, high emitted power is allowed, especially when telemetry is sought.

For the frequencies shown in Table 2, electromagnetic safety for avoiding effects from electromagnetic waves to humans is represented by Specific Absorption Rate, or SAR (W/kg). SAR is calculated inside biological tissues and is given by:

$$\text{SAR} = \frac{\sigma E^2}{2\rho} \text{ (W/kg)} \quad (20)$$

where  $\sigma$  and  $\rho$  are tissue conductivity (S/m) and density (kg/m<sup>3</sup>) respectively while  $E$  represents electric field magnitude. Standards for safety levels, with respect to human exposure to radiofrequency electromagnetic fields are provided in Table 3 [20, 21]. General public safety is usually considered.

**Table 3.** SAR safety levels (100 kHz–6 GHz)

Exposure conditions	General public SAR (W/kg) <sup>a</sup>	Persons in restricted environment SAR (W/kg) <sup>a</sup>
Whole body	0.08	0.4
(Local) head and torso <sup>b</sup>	2	10
(Local) limbs and pinae <sup>b</sup>	4	20

<sup>a</sup> Averaged over 30 min for whole body exposure and 6 min for local exposure.

<sup>b</sup> Averaged over any 10 g of tissue formed in cubical volume.

### 3. Investigation of $S_{21}$ link

#### 3.1. System efficiency under homogeneous environments

There is certainly an optimum efficiency that can be achieved by an antenna. There are several discussions around its definition. In order to achieve it, ideal environment can be considered. For example, in [6] a capsule antenna embedded in the middle of a three layer spherical phantom is examined. The three layers represent from center to surface, muscle, fat and skin tissues. It is verified that an optimum efficiency exists for such a small antenna (detained in a specific sphere of small radius) while maximum optimum efficiency decreases with sphere radius increase. Naturally, such an ideal environment can be hardly met. Still, the contribution of the work is significant since it shows that for deep implantation the optimum frequency becomes lower. It should not be forgotten however that the antenna electrical size is competing against physical size and therefore for lower frequencies (Medradio band of 400 MHz for example), the antenna electrical size needs to be very small leading to inefficient antennas but with less propagation losses because of the higher wavelength. On the other hand, the higher frequencies (of 2.4 GHz ISM band for example) allow for electrically larger and of higher efficiency antennas with the cost of higher body losses because of the smaller wavelength. This fact leads us to the observation that while general conclusions can be made for optimum frequency and antenna size, the  $T_x$ – $R_x$  pair should be always seen as a system where the system efficiency is obtained per case.

In [22] two identical directive wire dipole antennas are designed and used to investigate the link between them when they are both implanted inside a muscle tissue phantom (see Figure 3). Examined frequency region varies from 0.8 GHz to 2.8 GHz. Detailed comparison for a loss-less or lossy environment is carried out accompanied by measurements when the two antennas are embedded inside minced pork meat. As shown the achieved measured link (measured  $|S_{21}|^2$ ) is around  $-35$  and  $-40$  dB for 6 cm and 8 cm distance respectively and for the 1 GHz to 1.2 GHz frequency window where the antenna is also matched. Interestingly, as discussed in [22], a similar problem for a loop antenna and for a realistic phantom when the antenna is placed in several positions, reveals the in-body  $|S_{21}|^2$  to be around  $-50$  dB for the same frequency region [23], while in [24] and a 2.4 GHz bow-tie antenna link for a spherical three-layer phantom gives a  $-70$  dB result. As can be seen by the above results, the simulation scenario examined can reveal different results and, in that sense, each problem is unique. While general conclusions can be drawn, results can differentiate when parameters of the problem do change. Frequency can obviously differentiate the results. What is sometimes forgotten, however, is that antenna behavior and radiation mechanism can also affect the results. Antenna size can be a crucial parameter.

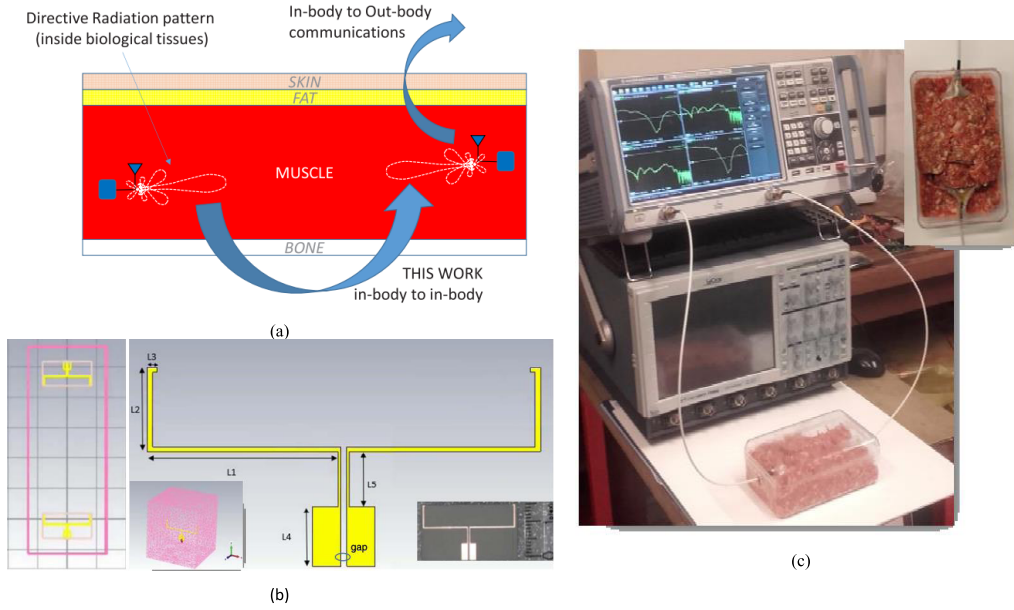


**Figure 3.** From [22]. Link simulation and measurements for two identical antennas inside tissue environment. (a) Problem under investigation; (b) directive antennas used in the simulation environment (dielectric muscle tissue box shown with pink color); (c) experimental measurement for minced pork meat.

**Table 4.** Implantable antennas tested for link estimation in scenarios of Figure 4

Antenna	Design/characteristics	Frequency of operation (MHz)	SAR <sub>1g</sub> (W/kg)	Volume (mm <sup>3</sup> )
“A” from [25]	Spiral, one layer	402–405	100	3457
“B” from [3]	Serpentine, one layer	402–405, 2.4–2.48	360 (402 MHz)	608
“C” from [26]	Stacked PIFA, double layer	402–405	300	336
“D” from [27]	Stacked, serpentine, double layer	402–405	660	33

### 3.2. System efficiency for complex environments

A computational experiment is carried out for four implantable microstrip antennas taken from [3, 25–27] whose details are shown in Table 4. Several other antennas could be considered. Microstrip antennas are usually chosen since they carry a ground plane and they can support the electronic circuitry on their back. The antennas of [3, 25–27] operate in the MedRadio band [14], at 402–405 MHz but they have different size and overall volume. In Figure 5d, the  $S_{21}$  link is investigated for a  $100 \times 100 \times 100$  mm<sup>3</sup> skin box between two identical versions of the antennas facing each-other at variable distances. As seen, the maximum  $S_{21}$  link variates from  $-25$  dB for the larger antenna to  $-50$  dB for the smaller antenna for a 20 mm in-between distance. The lowest link variates from  $-40$  dB to  $-85$  dB for 80 mm in-between distance.

While this distance falls in the near to medium field region, certain conclusions can be drawn. In comparison to [22] and for distance of 6 cm, maximum  $S_{21}$  value is at an almost equal value of  $-35$  dB. Notably, this happens for different frequencies with a ratio of 3:1. Of course, the antenna in [22] is intentionally designed to realize an implantable-to-implantable link and is relatively

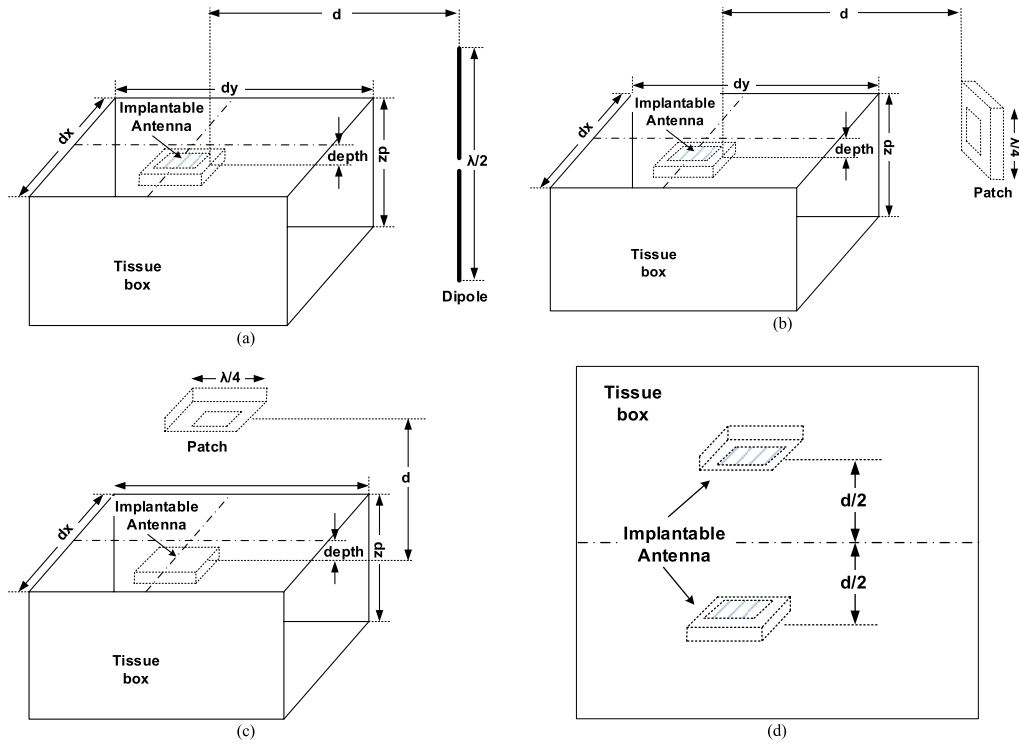


**Figure 4.** Implantable microstrip antenna (see Table 4) in a tissue skin box  $100 \times 100 \times 100 \text{ mm}^3$  and an external dipole or patch antenna at broadside or at the side of the implantable antenna. Tests (see Figure 5) were run for 402 MHz for the antennas from [3, 25–27] and included either the link calculation between the external and the implantable antennas (a, b, c) or between the implantable antennas (d).

electrically large. Electrical size can indeed affect efficiency. As shown in Figure 5d, the smallest antenna achieves multiple dB lower link as compared to its larger counterparts. In addition, the four tested antennas do not follow the same linear variation with distance in the calculated  $S_{21}$ . The antenna radiation mechanism and the boundary of the skin box can obviously affect the maximum achievable link. In addition, there might be an optimum frequency in relation to the antenna size and tissue properties for minimizing the internal losses [6].

In a homogeneous environment the frequency region of 900 MHz to 1.5 GHz could be the optimum one [6,7]. Still, as has been noted, the implantable antenna design can affect the results while the non-homogeneous environment has not been extensively studied.

It should be noted that the calculated  $SAR_{1g}$  in Table 4 is for input power of 1 W (30 dbm) and is naturally high. It has been provided for comparison between the different antennas. Still, as has been discussed in Section 2.3 maximum allowable power for implantable antennas varies. For example, at 400 MHz band (Medradio) maximum allowable power is  $-16 \text{ dbm}$  ( $25 \mu\text{W}$ ). In that case the results in Table 4 should be divided by 40,000 ( $=1 \text{ W}/25 \mu\text{W}$ ).

When the discussion moves to the link between an implantable antenna and an external antenna, different remarks could be drawn. Firstly, the implantable antenna far-field radiation properties need to be taken into account. Secondly, the external antenna type can also affect the outcome. Concerning the numerical experiment shown in Figure 4, a  $\lambda/2$  dipole or a  $\lambda/4$  rectangular patch are used as external antennas when the previously discussed microstrip

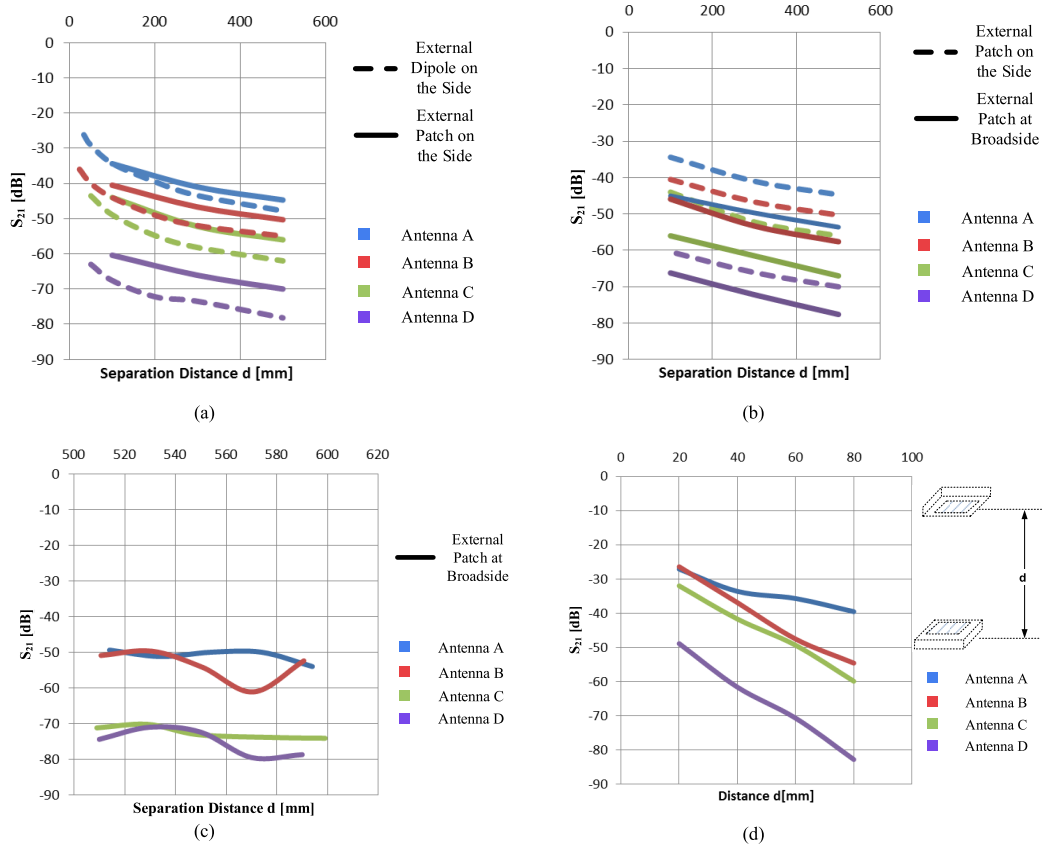


**Figure 5.**  $|S_{21}|^2$  (dB) for either an external dipole and/or a microstrip patch or two identical implantable antennas at  $f = 402$  MHz. Implantable antennas “A”, “B”, “C”, “D” are described in Table 4. Cases examined: (a) External dipole (Figure 4a) or microstrip patch (Figure 4b) on the side when the external antenna distance  $d$  variates and the implantable antenna is kept at depth = 5 mm; (b) External microstrip patch on the side (Figure 4b) or facing the implantable antenna (Figure 4c) when the external distance  $d$  variates and the implantable antenna is kept at depth = 5 mm; (c) External microstrip patch (Figure 4c) with implantable antenna when the external distance from the box surface is kept constant at 500 mm and the implantable antenna depth variates; (d) Identical antennas (A, B, C, D) immersed in the skin box, are facing each-other and their distance variates. Symmetry over box center is kept.

implanted antennas from [3, 25–27] (see Table 4) are immersed inside a  $100 \times 100 \times 100$  mm<sup>3</sup> skin box. Experiments include the placement of the external antenna on the side of the implanted antennas (Figures 4a,b) or at broadside facing each other (Figure 4c) and calculation of  $S_{21}$  link when the distance of the external antenna to the skin box surface varies (Figure 5a for external antennas on side and Figure 5b for comparison between patch on the side and at broadside) or when the external rectangular patch antenna is kept at fixed distance at broadside and the implantable antenna depth varies (Figure 5c).

External antennas were placed on the side because multiple miniaturized microstrip antennas operate at dipole mode. In that case, the optimum reception occurs when the external antenna

is on the side. For the numerical example investigated, even if we have not followed an optimum placement between the implantable and the external antenna on side, the link is higher. Indeed, for the frequency under investigation (402 MHz), when  $S_{21}$  from the external patch antenna on the side is compared against  $S_{21}$  from the patch antenna at broadside the link for the patch antenna on the side is 5 to 10 dB higher (see Figure 5b). The smallest difference occurs for the smallest implantable antenna. This result holds for distances from 100 mm to 500 mm.  $S_{21}$  varies almost linearly with the external antenna distance to the skin box surface.

For the same experiment, when we use the dipole and the patch antennas on the side, the  $S_{21}$  link is higher for the patch antenna (see Figure 5a). This is normally expected since the patch antenna has higher gain. Interestingly, the highest  $S_{21}$  difference is more profound for the smallest implantable antenna. Radiation pattern shape of the internal antenna may be the cause. In addition, the boundary effects of the skin box on the smallest antenna could create specific peculiarities. In any case this is another indication of the uniqueness of each case under investigation. Finally, when the external patch antenna is kept at fixed distance (at broadside for example—see Figure 5c), implantable antennas depth does not seem to affect the  $S_{21}$  link. This is obviously the outcome of the relative low frequency (i.e., 402 MHz) where the wavelength is relatively large. Since the external distance is kept constant, the internal “sub-wavelength” in-between variable distance does not influence the results. In that case, the implantable antenna volume (see Table 4) is a more crucial factor. Depending on the antenna design, skin box edge boundary also has an effect on the calculated results. In any case, it seems that, for larger distances of the external antenna or deeply implanted antennas, the lower frequency can offer a better link level.

Indeed, when the link between an implantable dipole and an external dipole antenna is examined and for several sub-GHz frequencies the same conclusion can be reached. Consider the problem shown in Figure 6. A simple tissue box is considered 100 mm in width, 100 mm in height, 50 mm in depth, filled with an equivalent tissue with relative dielectric permittivity equal to 2/3 of muscle. It should be noted that in several problems when homogeneous cubical phantoms are considered for representing the body, similar dielectric tissue is considered (for example see [3]). Two half-wavelength dipoles one implanted and the other in free space are considered and efficiency  $n'$  (see Equation (8)) denoted by  $G_a$  is calculated for a distance of up to 2 m. In Table 5, the frequencies tested are shown, in relation with dielectric properties used and the allowable power per frequency (see Table 2). First, as seen, the dielectric properties variate very little as is actually expected. Secondly, the permissible power increases with frequency. From Figure 6b we can see that obviously  $n'$  deteriorate much slower in the 400 MHz group of frequencies as compared to 868 MHz or 915 MHz. This is expected. When permissible power is taken into account and the achievable link is calculated from Equation (18) (here we consider that dipoles are well matched and therefore the denominator of  $n$  (Equation (8)) does not affect the final result, that is  $n$  and  $n'$  (Equation (6)) are practically the same), it is obvious that for every frequency a link can close (communication is successful) since every link is greater than the Required link of Equation (19). However, do not forget that we have considered maximum power emitted from the antenna. In that sense this link would be achieved if the  $T_x$  antenna was the external to the body. If we wanted to calculate what is the achievable link for an implantable antenna transmitting to an external to the body antenna, then SAR should have been calculated as has been also discussed above. In other words, while 915 MHz frequency can allow for sending information to an implantable antenna, the implantable antenna would be able to close a link at 400 MHz area where the fed power to the implantable antenna would not create excessive SAR. Furthermore if larger distances are to be considered, there is a point where the lower frequency can offer a better link, even for an external  $T_x$  antenna.

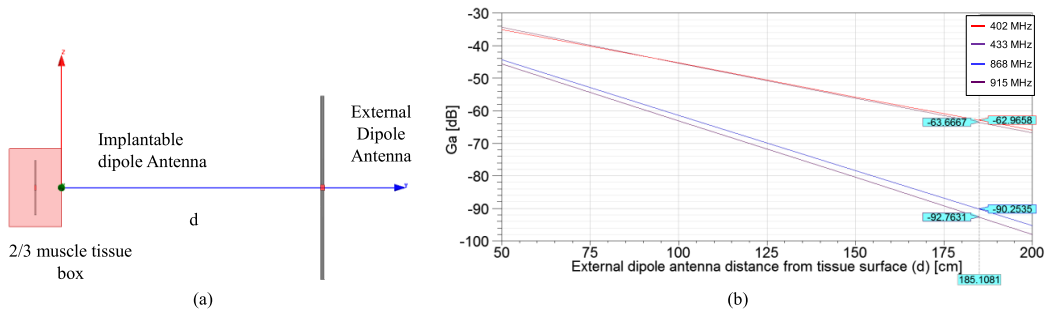


**Figure 6.** Simplified numerical test for  $n'$  efficiency (see Equation (8)) in (dB) (noted with  $G_a$ ) between an implanted half wavelength dipole inside a 2/3 muscle tissue type box and a free space half wavelength dipole at various distance and frequencies. Tissue box has 100 mm width, 100 mm height and 50 mm depth. The implanted dipole is placed at the box center (25 mm distance from surface).

**Table 5.** Frequencies tested, dielectric permittivity, allowed effective power and achievable link at 200 cm for the problem of Figure 6

$f$ (MHz)	Electrical properties of tissue-simulating model		ERP = Effective radiated power	Achievable link at 200 cm	Frequency band
	$\epsilon_r$	$\sigma$ (Si/m)	ERP <sub>max</sub> (dBm)	$C/N_0$ (Equation (18)) (dB/Hz)	Availability
402	38.07	0.53	-16	119.7	MEDS radio (worldwide)
433	37.91	0.54	10	124.7	ISM (Europe, Short range devices)
868	36.74	0.62	14	119.7	ISM (Europe, Short range devices)
915	36.66	0.63	30	133.7	ISM (USA and other parts of the world)

### 3.3. Antennas coupled with matching circuits: rectennas

For wireless harvesting systems, the antenna is coupled with a rectifier which is usually based on a combination of diodes and LC circuits. Other active elements might be also utilized. In that case the active circuit can be a part of scattering matrix. The circuit will have an output impedance equal to  $50 \Omega$ . However the antenna is not required to be designed at  $50 \Omega$  anymore. Hence, the receiver is a rectenna which is part of the scattering S matrix. In that case the system can be studied following the discussion in Section 2.1.1.

In [4], an implantable rectenna is obtained by combining an antenna (seen in Figure 8a) and a harvesting circuit at  $f = 915$  MHz. Defining the system efficiency as the ultimate criterion for the final rectenna system, after selecting the appropriate rectifier circuit the antenna implemented and the rectifier are combined, the circuit is optimized, and the rectenna is obtained. Antenna and the rectifier are studied as one system, and the antenna input impedance is not required to be matched at  $50 \Omega$ . A satisfactory efficiency is obtained while satisfying realistic conditions verifiable by measurements. It should be noted that at some proposed solutions in the literature, the obtained circuits are tested under high power which maximizes the efficiency. This is actually unrealistic due to the several design restriction of implantable systems.

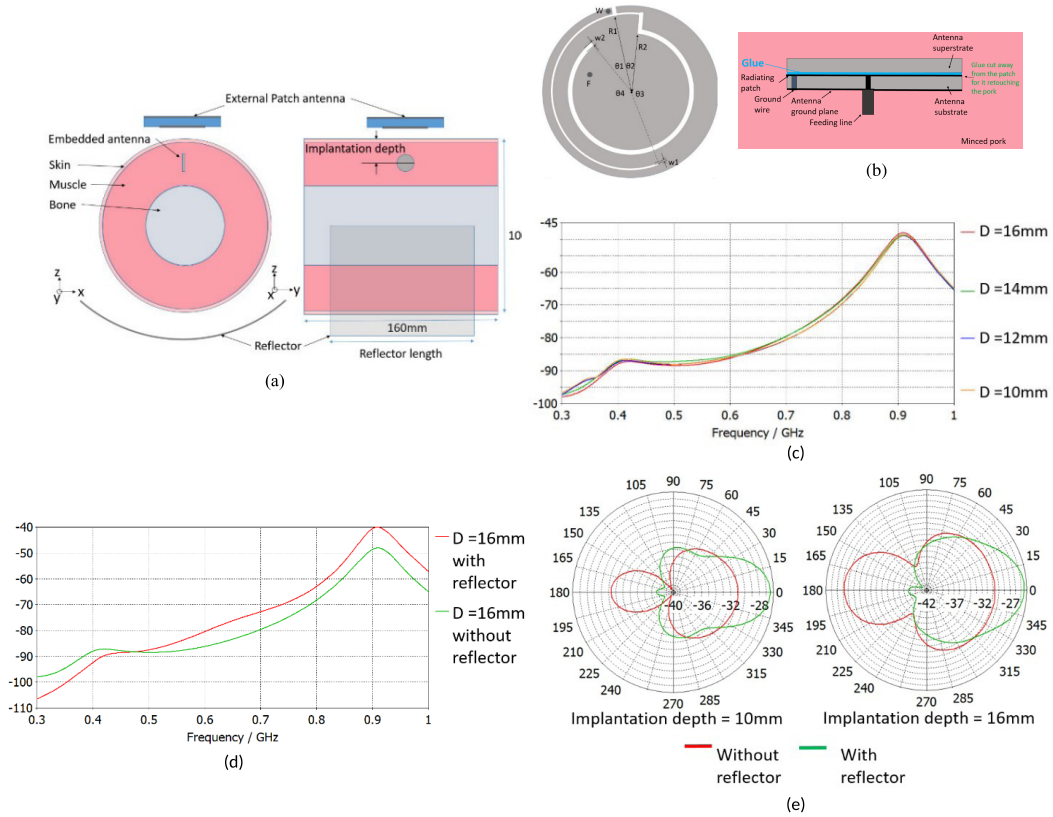


**Figure 7.**  $|S_{21}|^2$  (dB) between a minimized circular slot antenna implanted in a cylindrical arm phantom and an external patch antenna. Implantation depth varies from  $D = 10$  mm to  $D = 16$  mm. The external patch antenna distance from phantom surface is set at 200 mm. Implantable antenna volume is  $120 \text{ mm}^3$ . A cylindrical reflector can be also used for electromagnetic focusing as seen in (a). Results in (c) are without use of reflector while (d) ( $S_{21}$  link) and (e) (realized implantable rectenna gain) present the effect of reflector use. From [5].

In [5], an implantable rectenna system is obtained also at  $f = 915$  MHz. The antenna part of the system (see Figure 7) is extremely minimized. It is found that, taking into account the tissue environment, the antenna optimum performance is achieved at feeding port impedance  $Z = 110 \Omega$ . Therefore, the rectenna is built with this parameter in mind. System efficiency is again very good while a very small implantable rectenna is obtained. Results are verified against measurements.

### 3.4. System efficiency enhanced by external helpers

In implantable  $R_x$ - $T_x$  systems and in order to enhance the  $S_{21}$  link between the external and the internal antennas several external enhancements have been proposed. The most sophisticated, utilize the so-called metasurfaces which are usually applied on the skin covering an area relatively larger than the implantable antenna. Several examples can be found in literature. For example, in [28], a metasurface patch is proposed. Results show an enhancement of  $S_{21}$  link (implantable antenna reception) around 6 dB. The metasurface patch seems to operate as a focus lens.



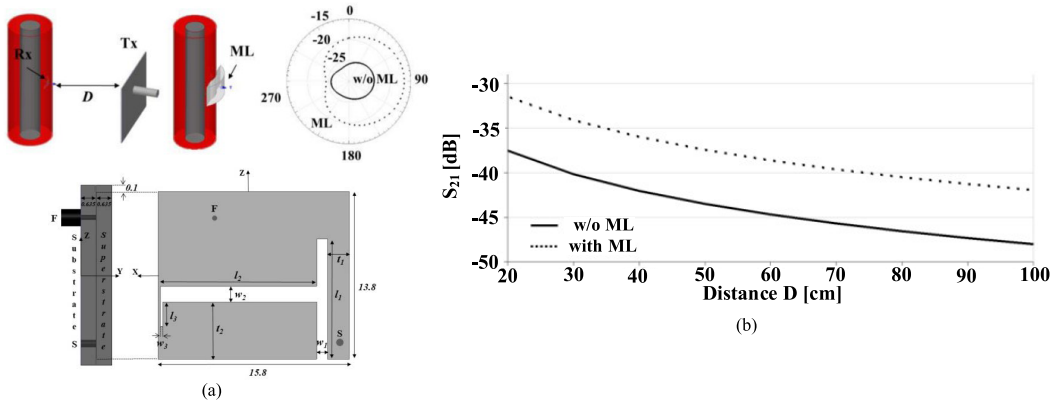


**Figure 8.**  $|S_{21}|^2$  (dB) between an implantable slot antenna at  $f = 915$  MHz and a rectangular  $\lambda/4$  patch antenna. Implantable antenna is embedded in a cylindrical arm phantom at 10 mm depth. It has a volume of  $285 \text{ mm}^3$ . A matching gel type ( $\epsilon_r = 20$ ,  $\tan \delta = 3 \times 10^{-3}$ ) denoted by ML is also used and it increases effectively the link. Results are extracted from [4].

Probably implantable antenna position can greatly affect the results and hence the system could be sensitive to misplacements. Similarly, in [29], an on-body metasurface is investigated. Up to 10 dB enhancements is reported. Still the size of the proposed metasurface could have large physical size. Its application on the skin could be sensitive to surface modification due to the body shape, etc.

Yet, enhancement can be achieved by implementing much simpler solutions which can have a similar effect. In [4], for an implantable rectenna coupled with an external antenna, a simple lubricating gel (appropriate for skin contact) with relative dielectric permittivity of  $\epsilon_r = 20$  and loss tangent equal to  $\tan \delta = 3 \times 10^{-3}$  is being used (system is shown in Figure 8). The gel can cover a small area, somewhat larger than the antenna aperture which is equal to  $14 \times 15$  mm and can effectively increase the achieved link by 6–7 dB as seen in Figure 8b. It is noted that the simulated results are verified by measurements [4]. As can be understood the gel application is not sensitive to misplacement or deformation because of the body shape and can offer a very simple but also effective solution for  $S_{21}$  link increase.

In [5], an alternative path is being proposed. The proposed implantable rectenna can be implanted in an arm (see Figure 7) while a curved metallic reflector is introduced in order to increase the link with an external antenna. The reflector is placed on the opposite side of the arm in relation with the external antenna. The reflector has a length of 16 cm, is placed at a 5 mm distance from the skin (to consider clothing) and covers the arm. As seen in Figure 7d, the reflector increases the  $S_{21}$  link by 7 to 8 dB. Simulated effect of reflector use, shown in Figure 7, has been also verified by measurements. While the reflector has a relatively large size, its application on the arm is very practical and can offer a robust solution for practical applications, insensitive as well to misplacement or arm shape.

#### 4. Conclusions

The design of an implantable antenna system that includes  $T_x$  and  $R_x$  components is governed by several parameters. While the operational frequency ranges from 400 MHz to usually 2.4 GHz or sometimes 5 GHz, depending on the application considered (e.g., communication between

or more implantable components, wireless transmission of medical data from an implantable sensor to an external hub, wireless control of an implantable system, wireless energy transfer) different factors can affect the final design. Since the outmost measure for an effective design is system efficiency, the external and implantable antennas can be considered as a system characterized by a scattering matrix. Calculation of  $S_{21}$  parameter is relatively simple and provides direct comparison with measurements. When a matching circuit is also considered either for antenna feeding or for using arbitrary load, this can be also considered as part of the system. Effectively,  $S_{21}$  can be used to cover several scenarios to obtain the optimum results. To that end, this paper, after determining  $S_{21}$  calculation for covering the above considerations, summarizes how the link budget can be obtained, what are the safety limits for implantable systems at frequencies of interest, and which are the allowable power for external or implantable antennas.

These factors are used to study a number of various scenarios, including  $S_{21}$  link calculation between either implantable antennas and/or implantable and external to the body antennas. Among others, this paper also show that while an optimum frequency, for example, can be determined for achieving an optimum link between two implantable antennas under ideal environments, different observations can be drawn when the antenna type, its design and the human phantom are considered. In addition, antenna size or how the antenna radiates can also define the link used. Telemetry cases where the external antenna can operate at its maximum power without violating safety limits are also considered. Interestingly, it is shown that while 915 MHz frequency allow for example much higher power use for an external antenna, when the distance of the external antenna from the body exceeds a limit then the use of a lower frequency with 20 dB less or lower power emission can actually secure a successful link. Finally, it is shown that while meticulously designed metasurfaces applied on the body have been proposed in order to enhance the link budget, much simpler and more robust solutions can be utilized.

In conclusion, the design of an implantable antenna is not exhausted by defining a minimum size or maximum gain. Many times, the  $T_x$  and  $R_x$  components need to be considered as a system and be investigated using scattering matrixes. This permits to investigate the effect of different parameters and concurrently offer a direct connection between simulations and measurements. Considering the design as a system can allow for generating, at the end, interesting results that will lead to an optimum, robust and well thought outcome.

## Declaration of interests

The authors do not work for, advise, own shares in, or receive funds from any organization that could benefit from this article, and have declared no affiliations other than their research organizations.

## References

- [1] M. Matthaiou, S. Koulouridis, S. Kotsopoulos, "A novel dual-band implantable antenna for pancreas telemetry sensor applications", *Telecom* **3** (2022), no. 1, p. 1-16.
- [2] W. G. Scanlon, B. Burns, N. E. Evans, "Radiowave propagation from a tissue-implanted source at 418 MHz and 916.5 MHz", *IEEE Trans. Biomed. Eng.* **47** (2000), no. 4, p. 527-534.
- [3] T. Karacolak, A. Hood, E. Topsakal, "Design of a dual-band implantable antenna and development of skin mimicking gels for continuous glucose monitoring", *IEEE Trans. Microw. Theory Tech.* **56** (2008), p. 1001-1008.
- [4] S. Bakogianni, S. Koulouridis, "A dual-band implantable rectenna for wireless data and power support at sub-GHz region", *IEEE Trans. Antennas Propag.* **67** (2019), no. 11, p. 6800-6810.
- [5] S. Ding, S. Koulouridis, L. Pichon, "Implantable wireless transmission rectenna system for biomedical wireless applications", *IEEE Access* **8** (2020), p. 195551-195558.

- [6] D. Nikolayev, W. Joseph, M. Zhadobov, R. Sauleau, L. Martens, "Optimal radiation of body-implanted capsules", *Phys. Rev. Lett.* **122** (2019), no. 10, article no. 108101.
- [7] D. M. Pozar, *Microwave Engineering*, Wiley, Hoboken, NJ, 2011.
- [8] C. Garcia-Pardo, A. Fornes-Leal, N. Cardona *et al.*, "Experimental ultra wideband path loss models for implant communications", in *2016 IEEE 27th Annual International Symposium on Personal, Indoor, and Mobile Radio Communications (PIMRC), Valencia, Spain*, 2016, p. 1-6.
- [9] R. Warty, M. R. Tofighi, U. Kawoos, A. Rosen, "Characterization of implantable antennas for intracranial pressure monitoring: reflection by and transmission through a scalp phantom", *IEEE Trans. Microw. Theory Tech.* **56** (2008), no. 10, p. 2366-2376.
- [10] Q. Chen, K. Ozawa, Q. Yuan, K. Sawaya, "Antenna characterization for wireless power-transmission system using near-field coupling", *IEEE Antennas Propag. Mag.* **54** (2012), no. 4, p. 108-116.
- [11] Y. Li, H. Sato, Q. Chen, "Capsule antenna design based on transmission factor through the human body", *IEICE Trans. Commun.* **101** (2018), no. 2, p. 357-363.
- [12] W. Xia, K. Saito, M. Takahashi, K. Ito, "Performances of an implanted cavity slot antenna embedded in the human arm", *IEEE Trans. Antennas Propag.* **57** (2009), no. 4, p. 894-899.
- [13] J. Zhang, R. Das, D. Hoare *et al.*, "A compact dual-band implantable antenna for wireless biotelemetry in arteriovenous grafts", *IEEE Trans. Antennas Propag.* **71** (2023), no. 6, p. 4759-4771.
- [14] "Medical Device Radiocommunications Service (MedRadio)", Federal Communications Commission. [Available in: <https://www.fcc.gov/medical-device-radiocommunications-service-medradio>].
- [15] ETSI EN 302 537 V2.1.1, "Ultra Low Power Medical Data Service (MEDS) Systems operating in the frequency range 401 MHz to 402 MHz and 405 MHz to 406 MHz; Harmonised Standard covering the essential requirements of article 3.2 of the Directive 2014/53/EU", 2016, European Telecommunications Standards Institute.
- [16] ETSI EN 301 839 V2.1.1, "Ultra Low Power Active Medical Implants (ULP-AMI) and associated Peripherals (ULP-AMI-P) operating in the frequency range 402 MHz to 405 MHz; Harmonised Standard covering the essential requirements of article 3.2 of the Directive 2014/53/EU", 2016, European Telecommunications Standards Institute.
- [17] "Wireless Medical Telemetry Service, 47 CFR Parts 1, 2, 15, 90 and 95", *Federal Communications Commission, Federal Register (The Daily Journal of United States Government)* **65** (2000), no. 137, p. 43995-44010.
- [18] ETSI EN 300 220-2 V3.2.2 (2024-03), "Short Range Devices (SRD) operating in the frequency range 25 MHz to 1,000 MHz with power levels ranging up to 500 mW e.r.p", [Available in <https://www.etsi.org/committee/1398-erm>].
- [19] 47 CFR Part 15, "Part 15. RadioFrequency Devices", [Available in <https://www.ecfr.gov/current/title-47/chapter-I/subchapter-A/part-15>].
- [20] ICNIRP, "Guidelines for limiting exposure to, electromagnetic fields (100 KHz to 300 GHz)", 2020, ICNIRP Guidelines.
- [21] IEEE C95.1-2019/Cor 2-2020, "IEEE standard for safety levels with respect to human exposure to electric, magnetic, and electromagnetic fields, 0 Hz to 300 GHz - Corrigenda 2", 2019-2020.
- [22] F. Mghar, A. Diet, C. Gannouni, L. Pichon, O. Meyer, S. Koulouridis, "Characterization of an intra-body wireless link in the UHF band", *Prog. Electromagn. Res. M* **111** (2022), p. 247-259.
- [23] A. Ibraheem, M. Manteghi, "Intra-body propagation channel investigation using electrically coupled loop antenna", *Prog. Electromagn. Res. M* **40** (2014), p. 57-67.
- [24] Y. El-Saboni, G. A. Conway, W. G. Scanlon, "Effect of tissue boundaries on the intra-body communication channel at 2.38 GHz", in *2017 International Workshop on Antenna Technology: Small Antennas, Innovative Structures, and Applications (iWAT)*, 2017, p. 285-288.
- [25] P. Soontornpipit, C. M. Furse, Y. C. Chung, "Design of implantable microstrip antennas for communication with medical implants", *IEEE Trans. Microw. Theory Tech.* **52** (2004), no. 8, p. 1944-1951.
- [26] C. M. Lee, T. C. Yo, C.-H. Luo, C. H. Tu, T. Z. Juang, "Compact broadband stacked implantable antenna for biotelemetry with medical devices", *Electron Lett.* **43** (2007), p. 660-662.
- [27] A. Kiourtis, M. Christopoulou, K. S. Nikita, "Performance of a novel miniature antenna implanted in the human head for wireless biotelemetry", in *IEEE AP-S International Symposium on Antennas and Propagation and USNC/URSI, Spokane, Washington, USA*, 2011.
- [28] S. Jo, W. Lee, H. Lee, "Metasurface patch for wireless power transfer in implantable devices", *Adv. Funct. Mater.* **33** (2023), no. 38, article no. 2300027.
- [29] N. Ghavami, E. Razzicchia, O. Karadima *et al.*, "The use of metasurfaces to enhance microwave imaging: experimental validation for tomographic and radar-based algorithms", *IEEE Open J. Antennas Propag.* **3** (2022), p. 89-100.